



## Comparative Study between Polyaniline and The Grafted Polyaniline with Chitosan and Their Application in The Removal of Hexavalent Chromium



I. El-Faramawy<sup>1</sup>, R. M. Sabry<sup>2</sup>, H. M. Ali<sup>2\*</sup>, N. S. Moursy<sup>1</sup>, F. A. Taher<sup>1</sup>

<sup>1</sup> Faculty of Science, Al Azhar University, Cairo, Egypt.

<sup>2</sup> Chemical Engineering and Pilot Plant Department, National Research Center, Dokki, Cairo, Egypt.

THE conductive polymer, polyaniline (PANI) and its grafting with chitosan (chitosan-grafted polyaniline, CS-g-PANI), were synthesized and analyzed by means of FTIR, TGA, TEM and XRD. The two resins were subjected for the adsorption of hexavalent chromium from aqueous solutions. The factors affecting the adsorption processes were tested, such as pH, time, temperature, and the initial concentrations of chromium. Also, both kinetics and equilibrium isotherm models were studied. The results indicated that the optimum conditions for the preparation of poly aniline are: APS to aniline ratio is 1.5, the HCL concentration is 2.5 M, the reaction time is 1.5h and the optimum ratio for the preparation of CS-g-PANI is 1.2. It was also found that the prepared nanoparticles of PANI may reach a size of 23–32 nm and the CS-g-PANI is 26–37 nm. The adsorption of chromium VI by the prepared polymers were found to follow Langmuire's isotherm with maximum adsorption capacity of 526 mg/g for PANI and 370 mg/g for CS-g-PANI at 60 °C. The adsorption mechanism was found to follow the second order model for the two products.

**Keywords:** Conductive polymer, Aniline, Chitosan, Nano-composite, Chromium removal.

### Introduction

In ancient and modern times, wastewater contaminated with heavy metals is considered one of the most important environmental problems that menace human life worldwide because of the movement of such impurities in aquatic ecosystem and the toxicity of these substances. With the continuous progress of industries like metal plating, mining, fertilizers, batteries, and tanneries industries, such metals are indirectly or directly discharged into aquatic environment [1,2]. The heavy metals are considered as stable environmental impurities because they cannot be decomposed and destroyed [3]. Based on these truths, the design and evolution of more effectual tactics for heavy metals elimination from industrial

wastewater is tremendously urgent for the future. These techniques comprising; ion-exchange, precipitation (physically and chemically), solvent extraction reverse osmosis and electrochemical treatment, are widely used methods to get rid of heavy metals found in industrial effluents [3]. However, these tactics are complex, expensive, and less efficient in some cases. Among various techniques for removing such pollutants from wastewater, adsorption process is known as one of the most effective and possible technique for water treatment [4,5]. The greatest benefits of the adsorption process are: It's simple in design, ease of operation, low initial cost and inattentiveness to poisonous pollutants. Moreover, it does not lead to the production of injurious substances [2, 6]. Natural polymers have been considered as an

\*Corresponding author e-mail: hanaa\_aly@hotmail.com

Received 27/11/2019; Accepted 22/12/2019

DOI: 10.21608/ejchem.2019.20096.2213

© 2020 National Information and Documentation Center (NIDOC)

environmentally friendly material because they are renewable, biodegradable, and non-toxic [7].

One of the best conducting polymers is polyaniline due to its monomer is inexpensive and can be simply polymerized with high yield at a low manufacture cost. Also, it has tunable features such as thermochemical stability and optical activity [8]. Owing to that, it can be used in numerous applications such as electrochromic, rechargeable batteries, supercapacitors, corrosion inhibitors, electromagnetic, biosensors, and have the ability to efficiently remove heavy metals and dyes.

However, the major drawback of these conducting polymers is the un-processability and intractability which has made their processing into the desired form is rather difficult. So, a number of approaches have been used to improve the poor mechanical properties of Polyaniline such as electrostatic deposition, graft copolymerization, or in situ polymerization of Polyaniline with different substrates. In situ polymerization of aniline with cellulosic substrates has been studied and provided composite with potentially useful properties [8,9, 10].

Chitosan (CS) is one of the natural polymeric materials which gained great attention nowadays because it is biodegradable, biocompatible, has high molecular weight, and low cost. In addition, the high reactivity of CS due to the presence of amine and hydroxyl functions simplify the modification of chitosan through the attachment to small or macromolecules [11,12].

CS and its derivatives have been established as adsorbents and ion exchange resins in water treatment due to the presence of the functional side groups which have the capability to adsorb pollutants by the formation of hydrogen bonding or electrostatic attraction [13,14].

Though, some weaknesses in the properties of CS such as, little stability and less de-fluoridation capacity (DC) of the raw CS limit its application as individual adsorbent [12]. The combination between CS and another polymer is one of the appropriate techniques used for the enhancement of the mechanical strength and increasing the sorption capacity

The main objective of the present study is to synthesize PANI as conducting polymer and CS graft with polyaniline copolymer by using an in situ chemical oxidation process. The type

of initiator, the molarity of HCL and reaction time will be studied for the preparation of PANI. While, the ratio between CS/ANI will be studied for the preparation of the grafted copolymer. The resulting products will be studied in the removal of hexavalent chromium from an aqueous solutions. The influence of pH, time and temperature on the removal efficiency was examined. Also, both equilibrium isotherms and kinetics models were tested.

## **Experimental**

### *Materials*

Aniline (ANI; Extra pure 99%), from LOBA Chem packed under Nitrogen. Ammonium per sulfate (Aps; Extra pure 98%), from OXFORD lobiem, INDIA). Chitosan (CS with high molecular weight 60000 by deacetylation 75 – 85 %), from HH Chemicals, Netherlands. Hydrochloric acid 36%, Acetic acid 96%, Diphenyl Carbazide from Win lab, UK. Acetone, Ultrapure 99% from Sigma cosmetic.

### *Experimental procedure*

#### *Preparation of Polyaniline*

1 mole of pure aniline was dissolved in known concentration of HCl (1, 2, 2.5, 3, 4, or 5 M). The required amount of ammonium per sulfate (Aps) salt was dissolved in HCl (2 M) and added dropwise to the aniline solution (different APS/ Aniline molar ratio 0.5, 1, 1.25, 1.5, and 2) then the reaction was kept under stirring at 750 rpm for 30 minutes then the precipitated dark green powder of PANI was filtered and washed by distilled water and acetone several times till the filtrate becomes colorless. The washed precipitate was dried at 60 °C and ground to fine powder in a mortar.

#### *Preparation of Chitosan/Polyaniline (PANI/CS) nanocomposite*

2.32 g of chitosan was dissolved in 2wt% glacial acetic acid solution, the required amount of aniline (0.05 M) was dissolved in HCl (2.5 M) to give different ratios of chitosan:aniline (0.5, 1, 1.2, and 1.5) then added to chitosan solution and stirring was continued at room temperature. 8.55 g of Aps salt was dissolved in HCl (2.5 M) and added drop by drop to the chitosan/aniline solution then the reaction was kept under stirring at 750 rpm for 90 minutes. The precipitated dark green powder of Chitosan/PANI was filtered and washed by distilled water and acetone several times till the filtrate becomes colorless. Finally the washed precipitate was dried at 60 °C and ground

to fine powder in a mortar. **Figure (1)** illustrates the reaction pathway for the synthesis of chitosan-grafted-polyaniline.

#### Fourier transform infrared (FTIR)

FTIR spectra were recorded on a Jasco FTIR-6100 system, using a pellet made with dehydrated KBr and instrument in the reflectance mode. FTIR spectra were recorded between 400 and 4000  $\text{cm}^{-1}$  with 4  $\text{cm}^{-1}$  resolution.

#### Electrical conductivity

The direct current electrical conductivity of the composites was measured by the four collinear probe technique using FOUR PROBE SET-UP Model: DFP-03 for a current source, voltmeter and temperature controller. Dry powdered samples were made into pellets using a steel die of 0.5 cm in diameter and 0.2 cm in thickness, pressed for 2 min in a hydraulic press under a pressure of (45 - 60) MPa.

The resistivity can be calculated by the following equation:

$$\rho = \frac{RA}{L} \quad (1)$$

Where ; R is the resistance of poly-aniline, A is the sample area & L is the distance between every two electrode 2 mm (constant).

Conductivity can be calculated using this equation :

$$\sigma = \frac{1}{\rho} \quad (2)$$

#### Transmission electron microscopy TEM

For TEM analysis, samples were prepared as a suspension in distilled water using sonication for 15 minutes, then drop was put on grid and images were taken on a JEOL (TEM-1230, Japan) electron microscopy, operating at acceleration voltage of 100 KV.

#### Thermal gravimetric analysis (TGA)

Thermograms of the polymers were recorded using a SDTQ600 thermal gravimetric analyzer in the presence of  $\text{N}_2$  atmosphere from 30 to 1000°C with a heating rate of 10°C  $\text{min}^{-1}$ .

#### X-ray diffraction (XRD)

XRD patterns were recorded using X-ray diffraction equipment model X-Pert PRO from 2  $\theta = 20$  to 60° using Cu- radiation ( $\lambda = 1.5418\text{\AA}$ ) at a scan speed of 0.04°  $\text{s}^{-1}$ .

#### Adsorption Experiment

Batch adsorption experiments of chromium were carried out to determine the adsorption capacities of the prepared resins (polyaniline and chitosan grafted polyaniline copolymer).

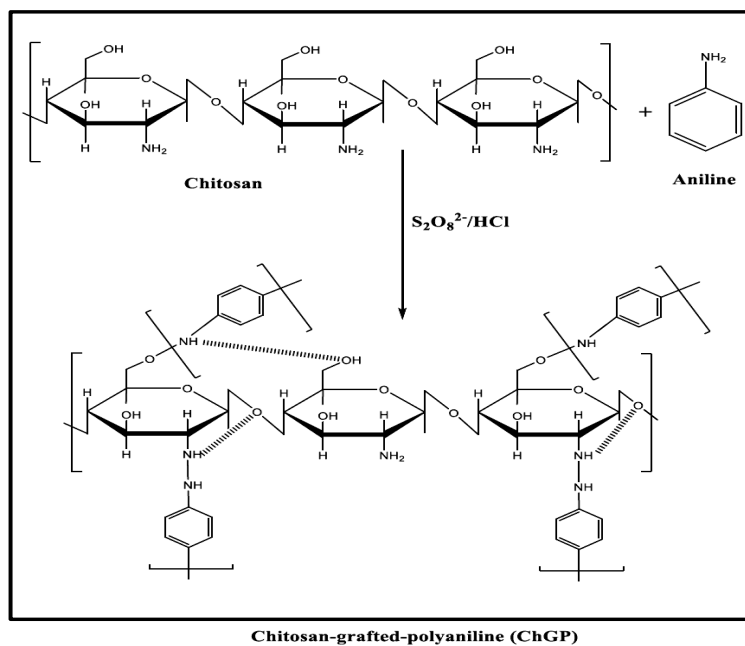


Fig. 1. The reaction pathway for the synthesis of chitosan-grafted-polyaniline 2.3. Analysis.

### *i. Effect of pH*

The effect of pH was carried out at chromium concentration 100 mg/l and solution volume 100 ml. The pH of the prepared solutions were adjusted in the range from 2 to 7 with 0.1N HCl or NaOH solutions. At each pH, 0.1 g of each resin was added to the respective pH solutions.

All the experiments were performed in an 250 ml Erlenmeyer flask, immersed in a shaker water bath (Julabo SW20), adjusted at 120 rpm agitation speed, for 24 hrs. The samples were then filtered, separated and analyzed for rejected chromium concentration by UV-Vis spectrophotometer at the wavelength 540 that corresponds to the maximum absorbance ( $\lambda$  max).

### *ii. Kinetic experiments*

At the optimum pH, the kinetics of adsorption of chromium onto the two adsorbents were carried out by withdrawing and analyzing the samples at the time interval of 5, 10, 20, 30, 45, 60, 120, 180, 300, 360 min and 24 hrs. The kinetic experiments were carried out for initial chromium concentration of 100 ppm at 15°C.

### *iii. Effect of temperature at different chromium concentrations*

The adsorption capacity of Chromium on the prepared resins at temperatures of 30, 45 and 60°C were performed by adding 0.1g of the resin to 100 ml of different concentrations of chromium solution (50 – 500 mg/l) at the optimum pH. The adsorption value was calculated by determining the adsorbate concentration before and after treatment, by means of the spectrophotometer. After equilibrium was attained, the metal uptake capacity for each sample was calculated according to a mass balance on the metal ion using equation (3) :

$$q_e = \frac{(C_0 - C_e)V}{m} \quad (3)$$

Where  $m$  is the mass of adsorbent (g),  $V$  is the volume of the solution (L),  $C_0$  is the initial concentration of metal ( $\text{mg L}^{-1}$ ),  $C_e$  is the equilibrium metal concentration ( $\text{mg L}^{-1}$ ) and  $q_e$  is the metal quantity adsorbed at equilibrium ( $\text{mg/g}$ ).

### *Adsorption Kinetic Models*

The kinetic study of adsorption in wastewater plays an important role because it affords important insight into the reaction pathways and into the mechanism of the reaction. Kinetic models have been proposed to explain the mechanism of

a solute sorption from aqueous solution onto an adsorbent :

- Pseudo first order kinetic model.
- Pseudo second order kinetic model.

#### *Pseudo-First Order Model*

The pseudo first-order kinetic model has been widely used to predict the metal adsorption kinetics. The metal adsorption kinetics following the pseudo first-order model is given by [15](Ho and McKay, 1999a):

$$\frac{dq}{dt} = k_1(q_e - q_t) \quad (4)$$

Where  $k_1$  ( $\text{min}^{-1}$ ) is the rate constant of the pseudo-first-order adsorption,  $q_t$  ( $\text{mg/g}$ ) denotes the amount of adsorption at time  $t$  (min) and  $q_e$  ( $\text{mg/g}$ ) is the amount of adsorption at equilibrium.

After definite integration by application of the conditions  $q_t = 0$  at  $t = 0$  and  $q_t = q_t$  at  $t = t$ , Eq. (4) becomes.

$$\log(q_e - q_t) = \log q_e - \left(\frac{k_1}{2.303}\right)t \quad (5)$$

By plotting  $\log(q_e - q_t)$  versus  $t$ , the adsorption rate can be calculated.

#### *Pseudo-Second Order Model*

The adsorption kinetic data can be further analyzed using Ho's pseudo second-order kinetics [16]. This is represented by :

$$\frac{dq}{dt} = k_2(q_e - q_t)^2 \quad (6)$$

Integration of Eq. (4) and application of the conditions  $q_t = 0$  at  $t = 0$  and  $q_t = q_t$  at  $t = t$ , give.

$$\frac{t}{q_t} = \frac{1}{(k_2 q_e^2)} + \frac{t}{q_e} \quad (7)$$

Where  $k_2$  ( $\text{g}/(\text{mg min})$ ) is the rate constant,  $k_2$  and  $q_e$  can be obtained from the intercept and slope.

#### *Adsorption Isotherm*

Adsorption equilibrium is established when the amount of solute being adsorbed onto the adsorbent is equal to the amount being desorbed [17]. The equilibrium adsorption isotherms were depicted by plotting solid phase concentration ( $q_e$ ) against liquid phase concentration ( $C_e$ ) of solute. Adsorption isotherm explains the interaction between adsorbate and adsorbent and is critical for design of adsorption process. The

Langmuir, Freundlich and Temkin isotherms are the most frequently used models to describe the experimental data of adsorption. In the present work these three isotherms were applied to investigate the adsorption process of chromium on the prepared resins at different conditions of process parameters.

#### Langmuir Isotherm Model

The Langmuir adsorption is the best model among the entire isotherm model and it is successfully applied in many adsorption processes. It is well known that the Langmuir isotherm is valid for monolayer adsorption on an energetically homogeneous surface [18, 19].

The parameters of Langmuir model can be calculated from the slope and intercept of the linear plot of  $C_e/q_e$  versus  $C_e$  that gives  $q_m$  and  $K_L$ .

The Langmuir equation is given by :

$$q_e = \frac{q_m K_L C_e}{1 + K_L C_e} \quad (8)$$

The linearization of equation (8) gives the following form:

$$\frac{C_e}{q_e} = \frac{1}{q_m K_L} + \frac{C_e}{q_m} \quad (9)$$

Where  $C_e$ , equilibrium metal concentration,  $q_m$  and  $K_L$  are the Langmuir constants related to maximum adsorption capacity (mg/g), and the relative energy of adsorption (1/mg), respectively.

#### Freundlich Isotherm Model

Freundlich isotherm model is one of the most widely used mathematical models which fit the experimental data over a wide range of concentration. This isotherm model is based on heterogeneous surface, distribution of active sites and their energies and enthalpy changes logarithmically.

The Freundlich equation is given by [20]

$$q_e = K_F C_e^{\frac{1}{n}} \quad (10)$$

The logarithmic form of equation is :

$$\ln q_e = \ln K_F + \frac{1}{n} \ln C_e \quad (11)$$

Where  $q_e$  is the amount of metal ion adsorbed after adsorption per specific amount of adsorbent (mg/g),  $C_e$  is equilibrium concentration (mg/L),  $K_F$  and  $n$  are Freundlich equilibrium constants.

#### Temkin Isotherm Model

Temkin isotherm contains a factor that clearly taking into the account of adsorbent-adsorbate interactions. The model assumes that heat of adsorption (function of temperature) of all molecules in the layer would decrease linearly rather than logarithmic with coverage on ignoring the extremely low and large value of concentration. Temkin isotherm is given by the following equation [21] :

$$q_e = \frac{RT}{b} \ln(aC_e) \quad (12)$$

Linear form of this model is given by the following equation :

$$q_e = a + b \ln C_e \quad (13)$$

Where  $q_e$  is the amount of metal ion adsorbed per specific amount of adsorbent (mg/g),  $C_e$  is equilibrium concentration (mg/L),  $a$  is equilibrium binding constant ( $g^{-1}$ ) and  $b$  is related to heat of adsorption (J/mol) which are Temkin constants.

#### Determination of the concentration of the chromium (VI)

The adsorption value was calculated by determining the adsorbate concentrations before and after treatment using DR 2800 spectrophotometer. Calibration curve for chromium was prepared by recording the absorbance values for a range of known concentrations of the chromium solution at its wavelength for maximum absorbance. ( $\lambda_{max} = 540$  nm) Plotting the absorbance against the concentrations gives a linear calibration curve passing through the origin as shown in **Figure (2)**.

## Results and Discussion

### Factors affecting the polymerization process

#### Effect of APS/ Aniline molar ratio on yield and DC conductivity

The synthesis is processed at molar ratios of 0.5, 1, 1.25, 1.5 and 2 in 2 M HCl and at constant time (30 minutes). As shown in **Figure (3)** the best APS/ANI molar ratio in yield and conductivity is 1.5. The increase in the yield% as the amount of initiator increases may be attributed to the increase of the produced sulfate ion radical moieties which activate the production of the PANI ion radical followed by the propagation of the polymer chain. The decrease in % yield as the initiator increases beyond this value may be due to the highly increase of the sulfate ions and free radical ions which may terminate the polymerization reaction than the propagation step.



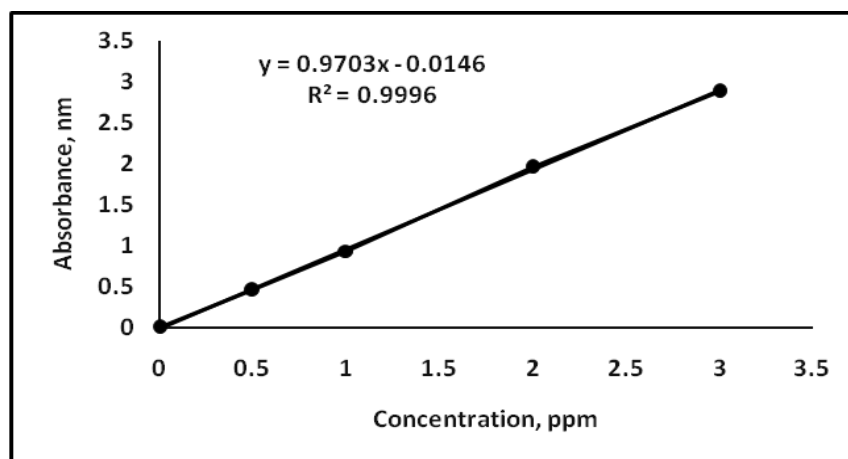


Fig. 2. Calibration curve of Cr.

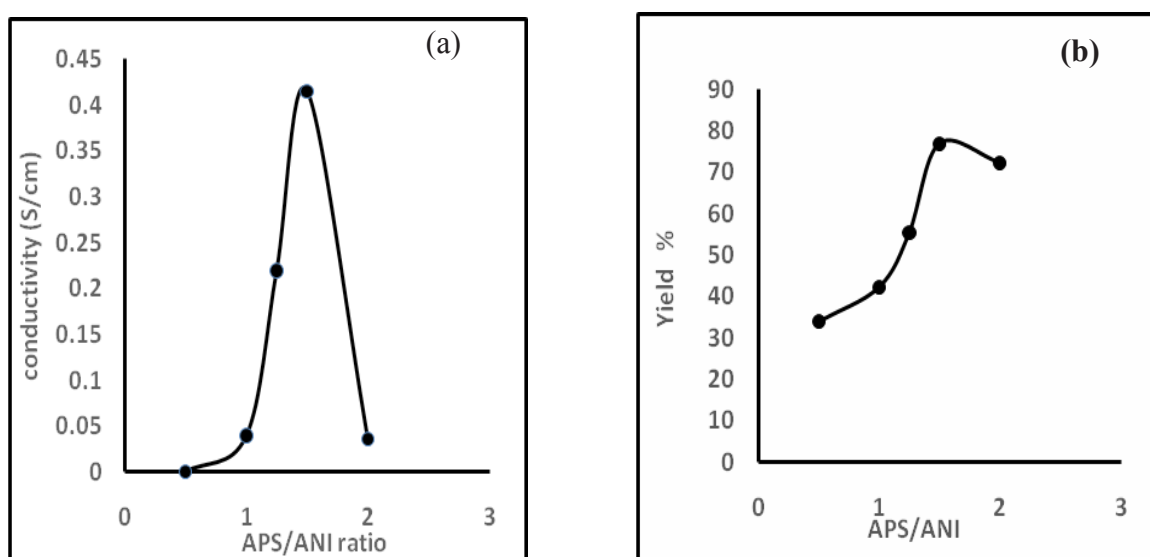


Fig. 3. Effect of APS/Aniline molar ratio on a) Conductivity and b) Yield at constant condition of 2M HCl and 30 min. reaction time.

#### *Effect of HCl molarity on yield and DC conductivity*

The synthesis is processed at the following HCl molarities; 1, 2, 2.5, 3, 4 and 5 at constant reaction time (30 min) and APS/ANI ratio = 1.5. As shown in **Figure (4 a & b)** the % yield was kept constant as the HCl concentration increases from 1M to 3M then it tend to decrease with the increase in HCl concentration. The increase of HCl concentration to 5M decreases the % yield of polyaniline this may be due to that some unescapable side reactions occur during the polymerization of aniline (**Figure 5**) involving the substitution of chlorine in aromatic ring [22].

From **Figure (4)** it was found that the conductivity of poly aniline was increased with

the increase of HCl concentration till 2.5M due to the increase of doping percentage. Then further increase of HCl concentration decreased the conductivity which may be attributed to substitution of chlorine in aromatic ring as represented in the previous paragraph [22]. So the best HCl molarity for the preparation of polyaniline is (2.5 M).

#### *Effect of polymerization Time*

The synthesis is processed at the following reaction time; 30, 60, 90, 120, 180 minutes at (2.5 M HCl) and APS/Aniline ratio = 1.5. As shown in **Figure (6 a and b)** the best time of polymerization on yield and conductivity is 1.5 hr.

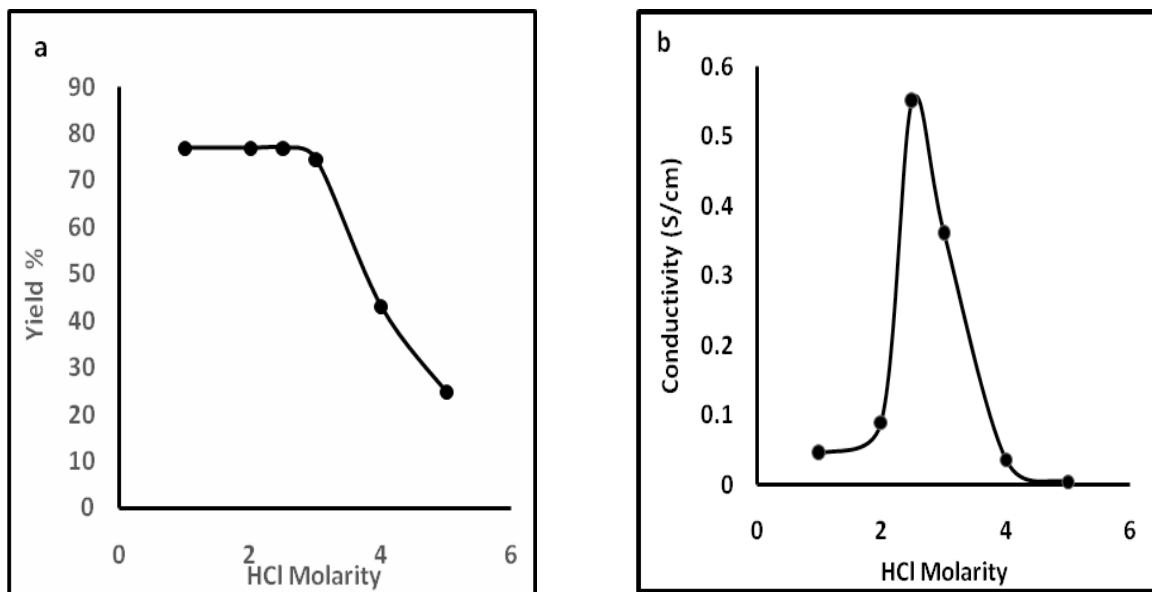


Fig. 4. Effect of HCl Molarity on a) Yield and b) Conductivity at 30 min reaction time and APS/ANI ratio = 1.5.

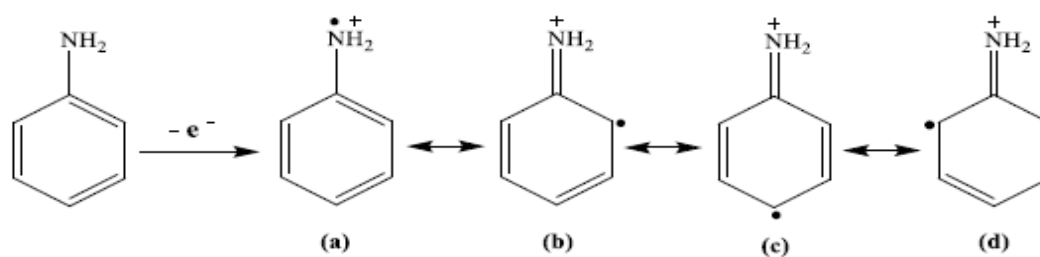


Fig. 5. Mechanism for the formation of aniline radical cation and its resonant structures.

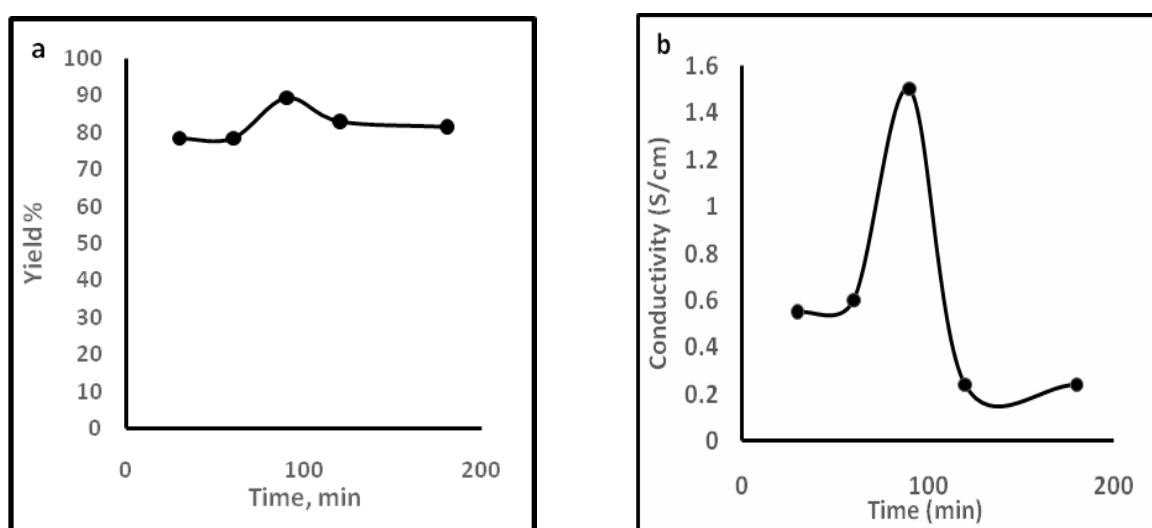


Fig. 6. Effect of Polymerization Time on a) Yield and b) Conductivity at 2.5 M HCl and APS/Aniline ratio = 1.5.

### Effect of CS/ANI molar ratio

The synthesis is processed at the following Chitosan/Aniline molar ratio; 0.5, 1, 1.2 and 1.5 at constant time 1.5 hr, temperature and molarity of HCl (2.5 M). From **Figure (7 a,b & c)** it is obvious that when the amount of aniline increases the graft yield decreases, so the highest yield is the ratio of CS/ANI = 0.5, but the conductivity decreased by increasing the amount of chitosan. Which means that conductivity of  $0.5 > 1 > 1.2 > 1.5$ . To find the optimum ratio between chitosan and aniline, the adsorption capacity of the prepared resin was examined. From **Figure (7c)** it was found that the highest capacity is at the ratio of CS/ANI = 1.2.

### Characterization of the prepared resins

#### FTIR results for PANI and Chitosan/polyaniline composite

The FTIR spectra of PANI, chitosan, and chitosan-grafted polyaniline nanocomposite are shown in **Figure (8)**. In **Figure (8a)** the spectrum of PANI shows that; the characteristic bands at 2925 and 2811  $\text{cm}^{-1}$  are owing to asymmetric

C-H extending and symmetric C-H stretching vibrations, respectively. IR bands at 1469  $\text{cm}^{-1}$  and 1589  $\text{cm}^{-1}$  represent the characteristic C-C stretching of benzenoid and quinoid rings in PANI, respectively. Band at 1295  $\text{cm}^{-1}$  is assigned to C-N stretching vibration of the secondary aromatic amine. bands at 1124 and 821  $\text{cm}^{-1}$  can be assigned to C-H in-plane and out of plane bending vibration of para di-substituted benzene ring, respectively [23,24]. IR spectrum of chitosan (**Figure 8b**) included the following; a band at 3441  $\text{cm}^{-1}$  that is owed to the extending vibration of O-H and the primary amine group (NH) groups. The bands at 2925, 2840, 1426, and 1360  $\text{cm}^{-1}$  are allocated to symmetric and asymmetric  $\text{CH}_2$  stretching vibration recognized to pyranose ring. Additionally, the band at 1632  $\text{cm}^{-1}$  is recognized for the C=O stretching in amide groups ( $\text{NHCOCH}_3$ ), due to the partial deacetylation of CH). Furthermore, the band at 1360  $\text{cm}^{-1}$  is ascribed to the C-OH vibration of the alcohol groups [25], while the bands at 1140 and 1031  $\text{cm}^{-1}$  are specific to C-O-C in glycosidic linkage [26].

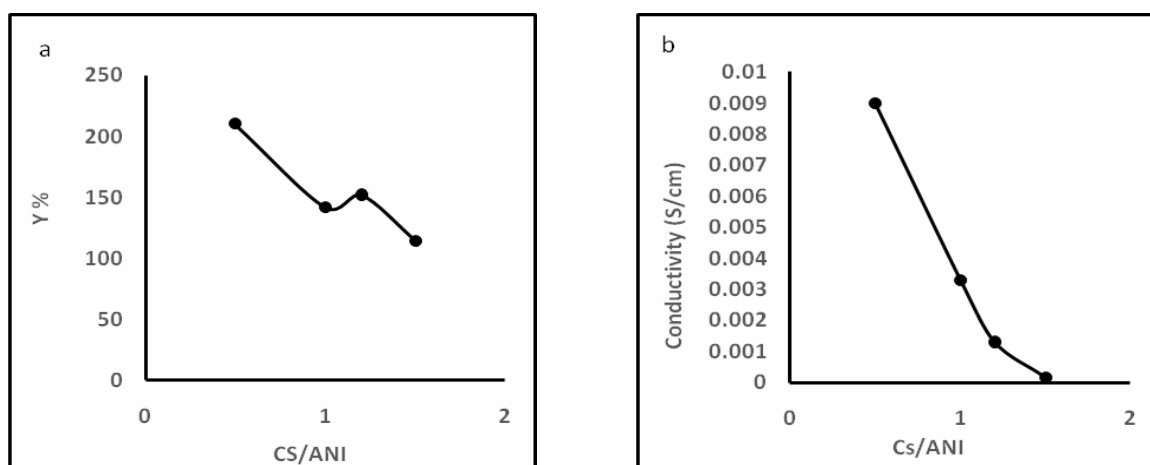


Fig. 7. Effect of Chitosan / Aniline Molar ratio on a) Yield and b) Conductivity at time 1.5 hr, and molarity of HCl (2.5 M).

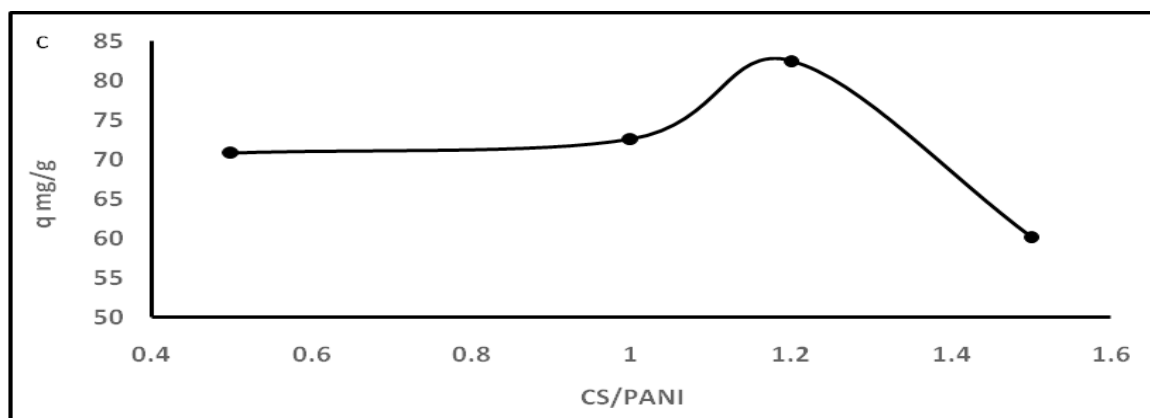


Fig. 7 c. Effect of adsorption of Cr (VI) into Chitosan / Aniline Molar ratios.



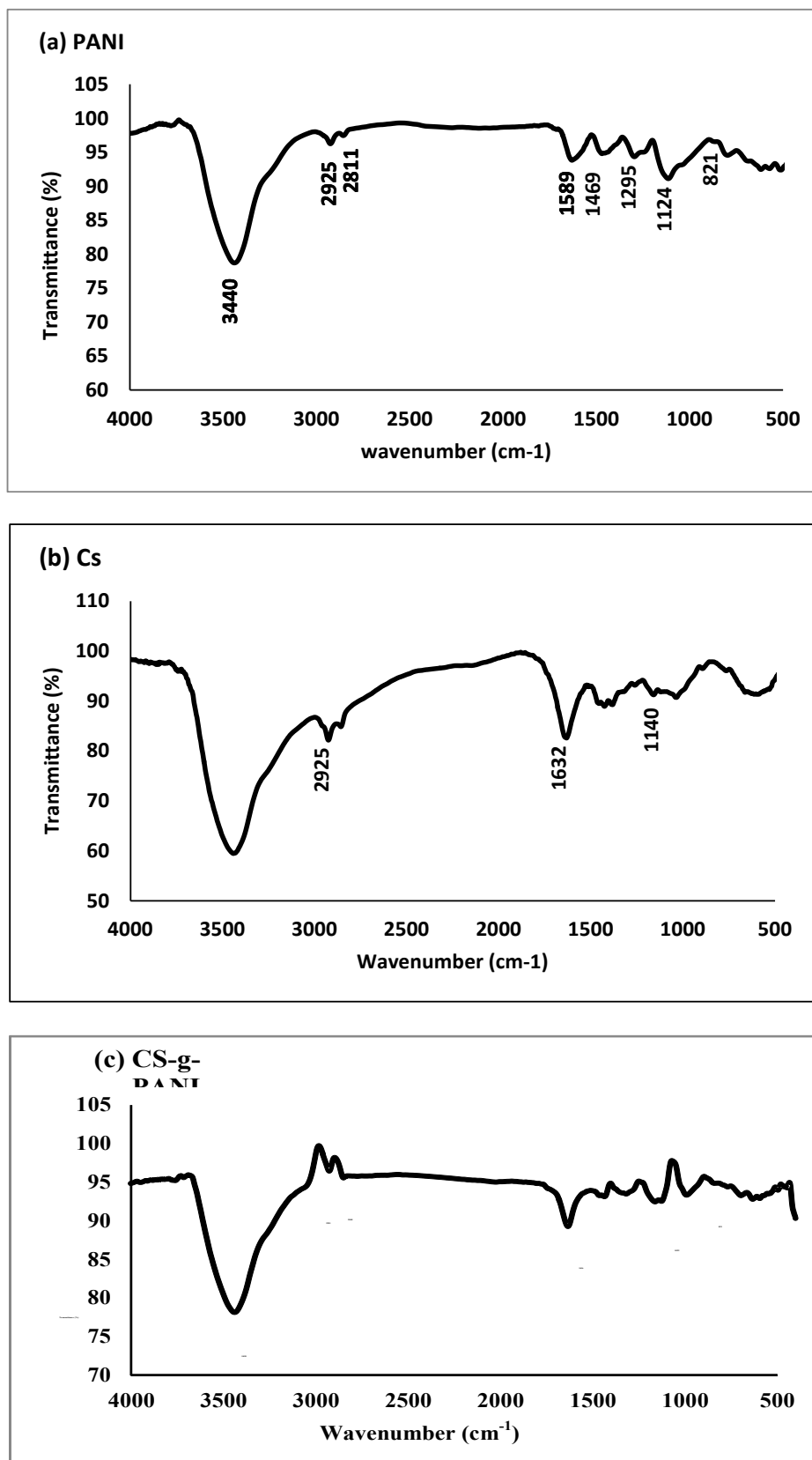


Fig. 8. FTIR spectra of a) PANI, b) Cs & c) CS-g- PANI graft copolymer.

IR spectrum of CS-g-PANI copolymer illustrates the specific bands of chitosan and PANI segments with some movements to the bands (**Figure 8c**). The intensities of the peaks at 2853 and 2923  $\text{cm}^{-1}$  increased representing the introduction of -CH groups, and the chitosan band at 1632  $\text{cm}^{-1}$  shifted to 1616  $\text{cm}^{-1}$ . Bands shifting at 3440 and 3441  $\text{cm}^{-1}$  in PANI and chitosan attributed to the hydrogen bonding between PANI and chitosan moieties (OH,  $\text{NH}_2$  and NH groups) as indicated by Khan *et al.*, 2009 [27]. Also, due to the overlapping of the N-H stretching of PANI and the -OH stretching of chitosan in graft copolymers, the IR band at 3440  $\text{cm}^{-1}$  became broad and less intense. This means that a substantial amount of O-H at chitosan has been grafted with polyaniline chains [28].

#### *Thermal stability of polyaniline (TGA of PANI and CS/PANI)*

The comparison between thermal stability of the graft copolymer (CS-g-PANI) and polyaniline (as a reference) was conducted by using of TGA analysis. **Figure (9a)** shows the thermal stability of PANI, the degradation of the polymer formed in four stages: the first stage losses 8.58 % of initial weight at temperature 30 up to 105 °C owing to the loss of moisture, elimination of impurities and unreacted monomers. Second stage from 105 to 345 °C, in which 25.16 % weight loss due to the loss of main polymer chain. Third stage 15.63% weight loss from 345 to 495 °C is occurred due

to side chain polymer loss. Final stage at 1100°C, about 11.19% of initial weight was remained as a residue. While, the thermal stability of CS-g-PANI copolymer shows the degradation of CS-g-PANI in three stages (**Figure 9b**), as can be seen the polymer begins to soften from the temperature of about 100 °C, and continues to 228 °C. This issue is caused by the loosening of connection between PANI and CS. At this point (the first stage), the polymer loss 28.27 % of initial weight due to the loss of moisture and solvent of polymer. Degradation begin at 228°C and continues to 300 °C. This is (the Second stage) causes 16.54 % mass reduction. At the third stage from 300 to 1000 °C, this is associated with the loss of main polymer chain with 17.43% loss of weight. Finally, at end of experiment at 1000 °C, 37.76 % of initial weight of CS-g-PANI composite was remained as a residue. As a result, the graft copolymer indicated higher thermal stability than pure PANI. It indicates that CS-g-PANI is more thermally stable than aniline.

#### *TEM (Transmission Electron Microscopy)*

**Figure (10)** represents the TEM images of the synthesized PANI and PANI-Cs nanocomposite. From these images, it is evident that PANI particles are mostly spherical in shape with average diameter of 23–32 nm (**Figure 10a**), while CS-g-PANI graft copolymer show granular structure in a shape looks like leaves with average diameter of 26–37 nm (**Figure 10b**).

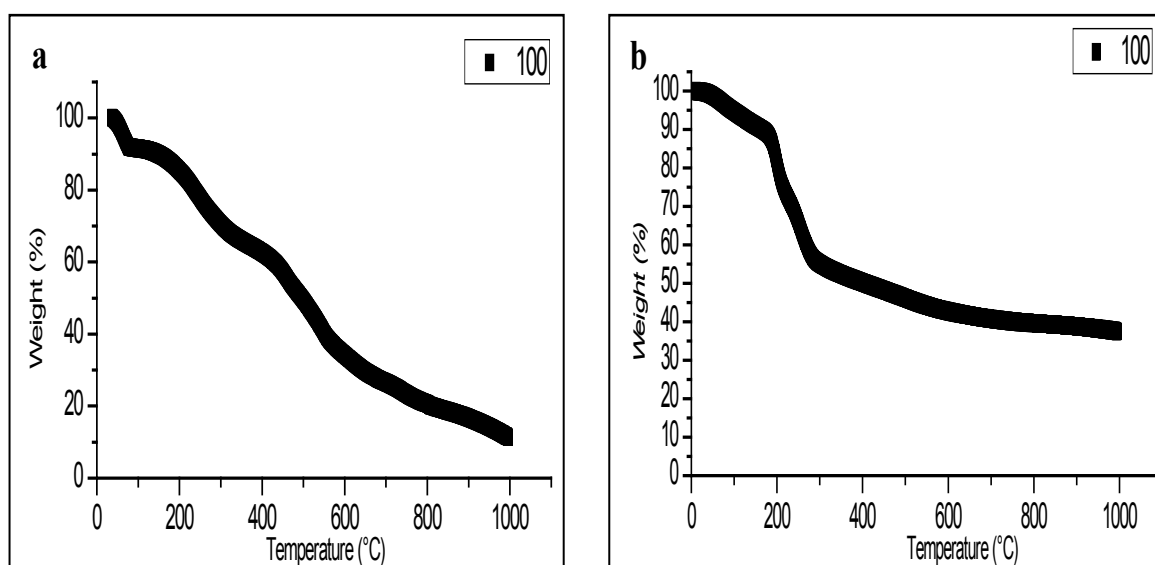


**Fig. 9.** TGA of a) PANI and b) CS/PANI nanocomposite.

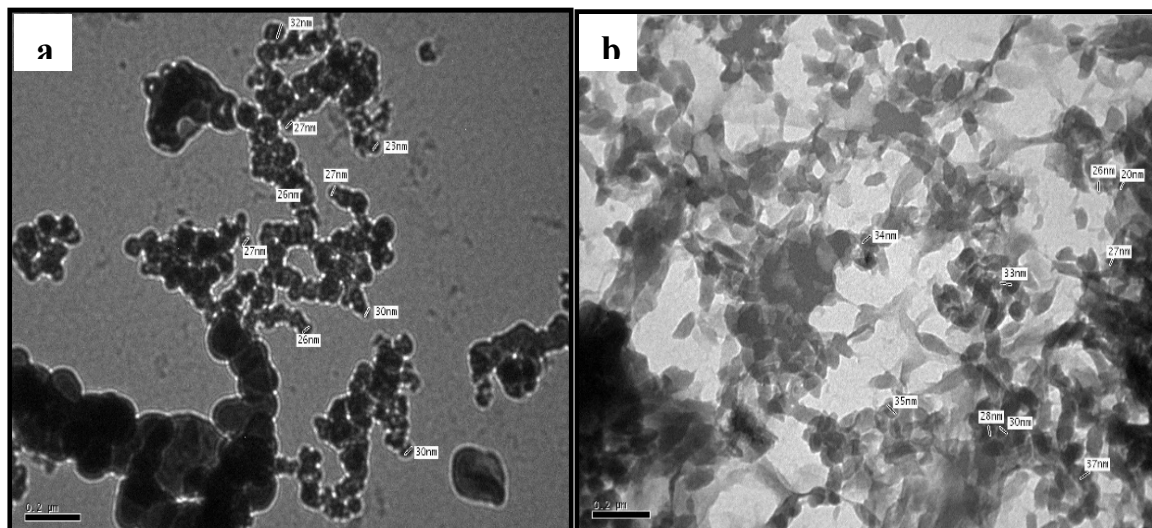


Fig. 10. TEM images of a) PANI and b) CS-g-PANI nanocomposite.

#### XRD analysis

Figure (11) shows the XRD patterns of PANI, CS and PANI/CS. For PANI the characteristic peaks located at  $2\theta = 19.1798^\circ$  and  $2\theta = 25.2639^\circ$  with a d spacing  $4.62761 \text{ \AA}$  and  $3.52529 \text{ \AA}$ , respectively, which displays low crystallinity of the conductive polymers because of the repetition of benzenoid and quinoid rings in PANI chains [29]. Chitosan shows the two distinct major crystalline peaks at  $2\theta = 10.7216^\circ$  and  $20.09^\circ$  due to existence of hydroxyl and amino groups in the chitosan structure [30]. In case of CS-g-PANI the peak at  $10.7216^\circ$  disappeared and the peak at  $20.09^\circ$  decreased sharply and the very broad peak was occurred at  $2\theta$  from  $18\text{--}26^\circ$  which suggests the grafting of PANI on a chitosan backbone [31]. Also, the decrease in crystallinity may be owing to the PANI side chains being introduced onto chitosan main chains [32].

#### BET (Brunauer, Emmett and Teller):

As illustrated in Table (1) the surface area of PANI is higher than that of CS-g-PANI copolymer by about  $3 \text{ m}^2/\text{gm}$ , this means that PANI may have more adsorption characteristic than CS-g-PANI graft copolymer.

#### Application of the prepared resins in the removal of Cr (VI)

This section will be devoted to the study of the main parameters affecting equilibrium isotherms and kinetics of the adsorption process.

#### Effect of pH

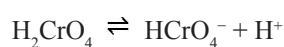
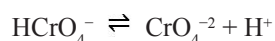
It is well-known that pH is one of the essential factors which influence the adsorption processes [33]. Figure (12) presents the effect

of pH on the adsorption capacity of Cr (VI) from aqueous solution by CS, PANI and PANI-CS. At 0.1 g of resins, 100 ml Cr (VI) solution with concentration 100 mg/L, temperature  $15^\circ\text{C}$  and 120 rpm. The results indicated that the highest removal of Cr (VI) occurs at pH 3 for CS, and pH 2 for PANI, and CS-g-PANI graft copolymer.

In low pH's, the nitrogen atoms of PANI are protonated to be  $(\text{NH}^+)$ . Conversely, the chromate ions are anions. So, the adsorption takes place during the electrostatic interaction between the counter ions. Thus, increasing of pH resulted to depletion of active sites especially in the PANI segments.

For PANI and CS-g-PANI, within the studied pH range (2–6) used in the present work, the capacity of the resins is slightly decreases with increasing pH from 2 to 6 with maximum capacity at pH 2. Such result is in agreement with Karthik, [34] result who found that the best absorption of Cr(VI) by CS/PANI composite at pH 2.

In the range of pH from 1 to 6 there are various forms of Cr exist, for example: hydrogen chromate ( $\text{HCrO}_4^-$ ) and dichromate ( $\text{Cr}_2\text{O}_7^{2-}$ ), being  $\text{HCrO}_4^-$  the major species, while at pH higher than 6,  $\text{CrO}_4^{2-}$  is more predominant. The Cr(VI) speciation is based on pH of the solution, as indicated from equations [34]



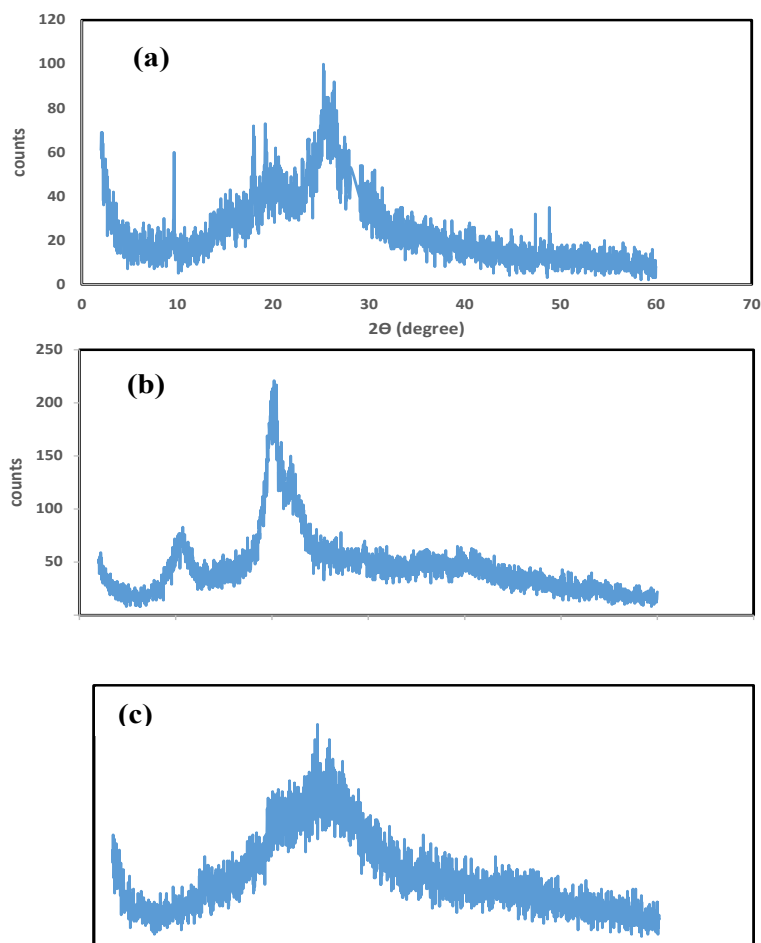


Fig. 11. XRD pattern of a) PANI, b) Cs & c) PANI-Cs graft copolymer.

TABLE 1. Surface area of PAN and CS/PANI copolymer.

Nano-material	Surface area $m^2/g$
Poly-aniline polymer	27.6444
CS/PANI nanocomposite	24.3221

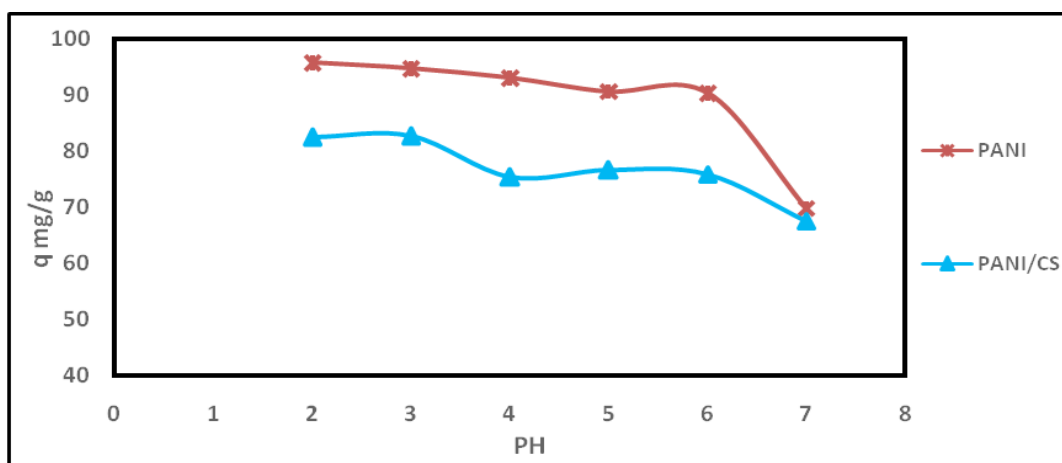


Fig. 12. Effect of pH on adsorption of Cr (VI) onto PANI, Cs and PANI-Cs nanocomposite.

For chitosan whose pKa 6.3 to 7.2 [34], at pH less than 6, the  $\text{NH}_2$  and  $\text{OH}$  groups at the molecules of chitosan are completely protonated ( $\text{NH}_3^+$  and  $\text{OH}_2^+$ ), leading to the presence of highly positive charge which utilizes strong attraction with the negatively charged  $\text{Cr(VI)}$  ions. But, by increasing the pH, the number of sites with positive charge decrease and the adsorption capacity will decrease. Also, the competition of the  $\text{OH}^-$  and  $\text{HCrO}_4^-$  anions available in the medium to be adsorbed on the solid surfaces [35] will decrease the adsorption capacity.

#### Effect of contact time.

Figure (13) shows that the removal of ions was increased with increasing in the contact time. The results indicated that  $\text{Cr(VI)}$  removal was increased to 49% and 34% by PANI and CS/PANI respectively, within the first five minutes. From 5 to 60 minutes, the capacity of  $\text{Cr(VI)}$  by PANI was increased slowly to be (58%), while the capacity of  $\text{Cr(VI)}$  by PANI-CS was increased in

fast rate to reach (62%). The percentage removal of  $\text{Cr(VI)}$  by PANI was increased in a fast rate to be (82%) when the contact time increased from 60 to 360 minutes, while the percentage removal of  $\text{Cr(VI)}$  by PANI-CS was increased in a very slow rate to reach 68%. The equilibrium was reached after 24 hrs by slight increase in capacity to 95.8%, 82.5% for PANI and CS-g-PANI.

#### Effect of temperature

Figure (14 a and b) indicates that the adsorption capacity of the two resins increased by increasing the concentration of the chromate ions until reached the equilibrium conditions. With increasing temperature, the capacity of the adsorbents increase due to endothermic process of the diffusion process and an increase in temperature increases the diffusion rate of the adsorbate molecules across the external boundary layers and into the pores of the produced polymers. The same behavior was found by [36,37].

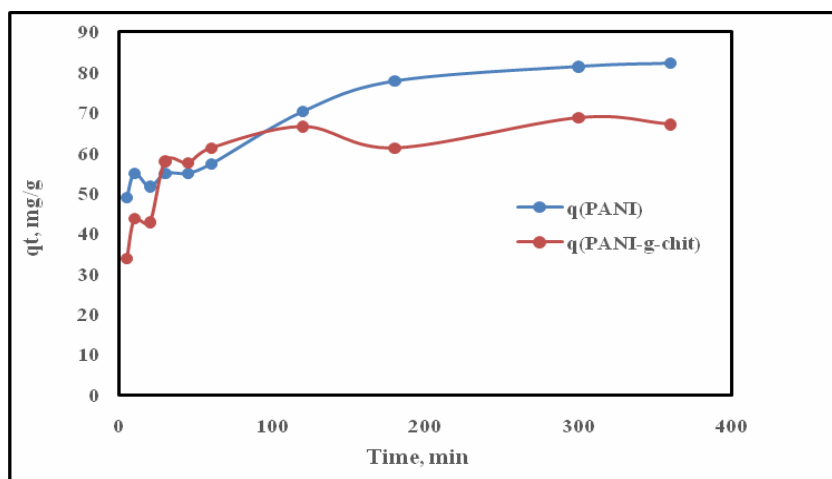


Fig. 13. Effect of contact time on the adsorption of  $\text{Cr(VI)}$  by PANI & CS-g-PANI.

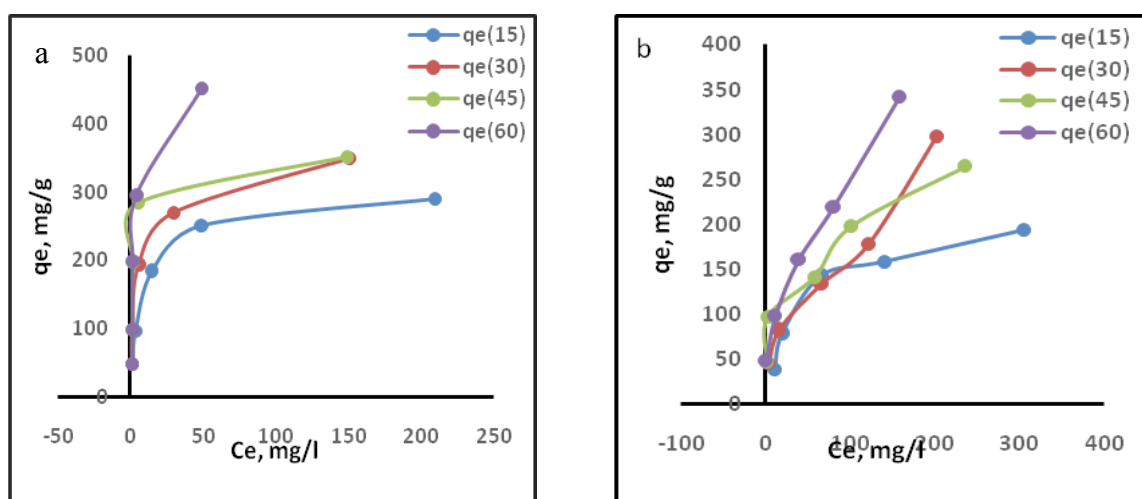


Fig. 14. The adsorption capacity of the two resins at different temperatures (a) PANI and (b) Cs-g-PANI.

### Sorption Kinetics Models

The simulation of the obtained experimental data was tested by two kinetic models (pseudo first order and pseudo second order kinetic model) as shown in **Figure 15 (a & b)**.

The calculated parameters from the two kinetic models from their own plots (Figure 12) are reported in **Table 2**. From the correlation coefficient values ( $r$ ), the results recorded that the kinetics of the Cr (VI) adsorption on PANI and CS-g-PANI composites was labeled well by pseudo-second-order model. So, the adsorption of chromate ions into either of polyaniline or chitosan grafted polyaniline were chemisorption

processes and controlled by the adsorption rate not the mass transport rate [38,39].

### Adsorption Isotherm

Heavy metal adsorption is usually modelled by the classical adsorption isotherms. Through the present study, three isotherms models (Langmuir, Freundlich, and Temkin isotherms) were applied using equations (9), (11) and (13) respectively at different initial metal ion concentrations (50, 100, 200, 300 and 500). In order to show the effect on initial concentration of Cr (VI) on removal efficiency PANI and CS/PANI, five different initial concentrations were used. The calculated values of the applied models were reported in Table 3.

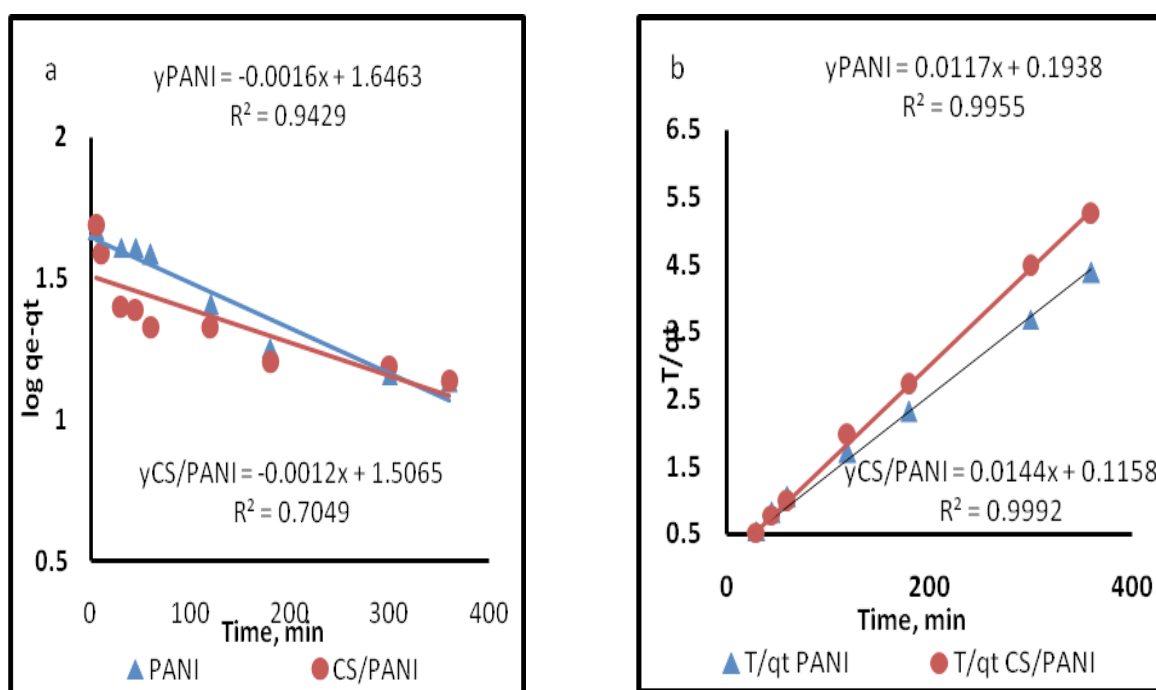


**Fig. 15.** The kinetic models Pseudo first order (a) and Pseudo second order (b) plot For the adsorption of chromium ions.

**TABLE 2.** Calculated parameters of the two kinetic models.

Resin	Pseudo-first-order		Pseudo-second-order	
	$K_1$ ( $\text{min}^{-1}$ )	$r^2$	$K_2$ ( $\text{g/mg min}$ )	$r^2$
PANI	3.7914289	0.9492	$7.063 \times 10^{-4}$	0.9955
CS/PANI	3.4694695	0.7049	$17.90 \times 10^{-4}$	0.9992



## i) Langmuir model

**Figure (16)** represents the fitting of the experimental data of the chromium removal by PANI with the linear form of Langmuir model.

The relation between  $C_e/Q_e$  and  $C_e$  gives a straight line over the entire concentration range with a slope of  $1/q_m$  and an intercept of  $1/q_m K_L$  (**Fig. 16**). The calculated values of the correlation coefficient ( $R^2$ ) are reported in Table 1 for both PANI and CS-g-PANI. The high values of  $R^2$  indicated that the adsorption process follows the Langmuir model for the two resins especially for PANI which gives correlation factor close to 1. The maximum adsorption capacity of PANI is 526 and 370 mg/g for CS-g-PANI, this obviously indicated that PANI has higher affinity for Cr(VI) ions than CS-g-PANI copolymer.

## ii. Freundlich isotherm model

Using equation (11), a straight line was obtained by plotting  $\log q_e$  against  $\log C_e$  (**Fig. 17**). The intercept of the line gave the  $\log K_f$  and the slope is  $1/n$ .

**Table 4** recorded the numerical value of  $n$  which is more than 1 for all adsorbents reported a good adsorption process [40]. The higher correlation coefficient for CS-g-PANI shows that the adsorption of Cr(VI) ions onto this resin is more adequate than onto PANI. This isotherm also predicted a multilayer adsorption of the Cr(VI) ions on the surface of CS-g-PANI than PANI.

## iii. Temkin isotherm model

By plotting  $q_e$  versus  $\ln C_e$  (**Fig. 18**), the constant  $b$  can be obtained from the slope,  $RT \ln A$  from the intercept,  $RT \ln A$ . From **Table 5**, the highest correlation coefficient ( $R^2$ ) for the Temkin isotherm was found to be 0.98 and 0.966 for PANI at low temperature (15 and 30°C) but they were lower than that of Langmuire correlation (0.9999 and 0.9983) which means that most of the experimental data fit very well Langmuire model.

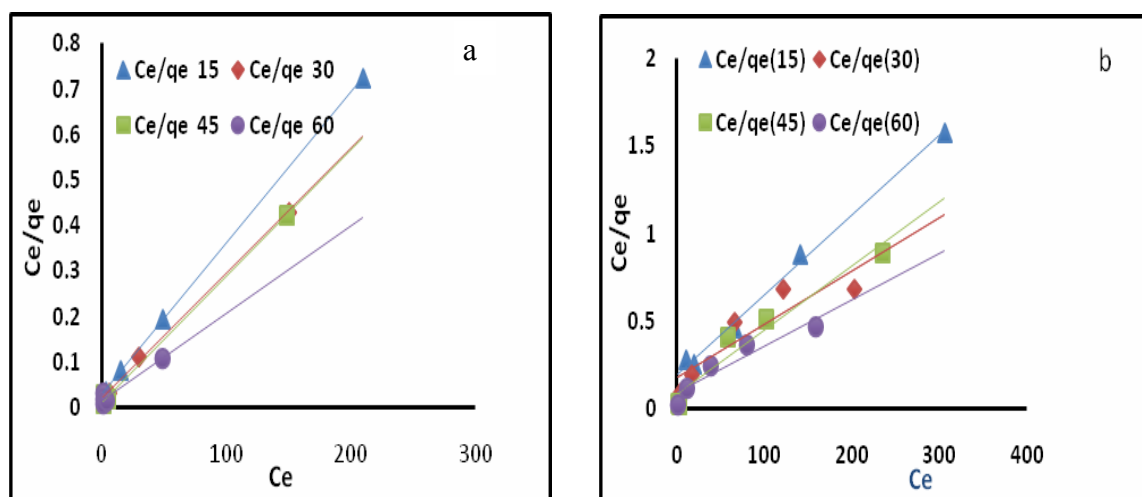


**Fig. 16.** Langmuir isotherm model for Cr adsorption onto (a) PANI and (b) CS/PANI.

**TABLE 3.** Langmuir adsorption isotherm parameters.

Polymer	T°C	$K_L$ (l/g)	$A_L$ (l/mg)	$q_{max}$ (mg/g)	Correlation coefficient $R^2$
PANI	15	0.10714	.01092	333.33	0.9999
	30	0.1459	0.021672	370.37	0.9983
	45	0.2745	0.0137	357.14	0.9981
	60	0.1397	.015	526.32	0.9484
CS/PANI	15	0.0237972	.0062	217.39	0.9952
	30	0.0168161	.035	333.33	0.8148
	45	0.045565	.030713	270.27	0.949
	60	0.0306122	.03066	370.37	0.8929

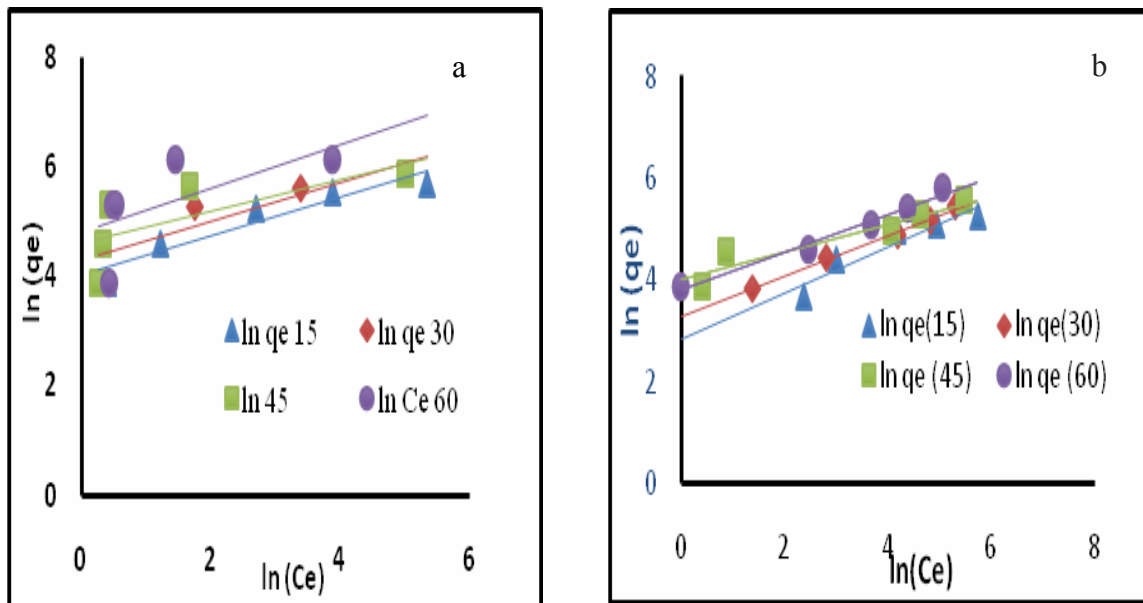


Fig. 17. Freundlich isotherm model for Cr adsorption by (a) PANI and (b) CS-g-PANI.

TABLE 4. Freundlich adsorption isotherm parameters.

resin	T°C	$K_f$ (l/g)	n (-)	Correlation Coefficient $R^2$
PANI	15	55.45	2.829	0.8966
	30	72.038	2.8167	0.8201
	45	101.464	3.51617	0.5004
	60	120.9164	2.5125	0.4148
CS/ PANI	15	17.279	2.221728	0.8975
	30	26.531	2.506265	0.9965
	45	55.757	3.687315	0.8855
	60	44.7	2.69396	0.9755

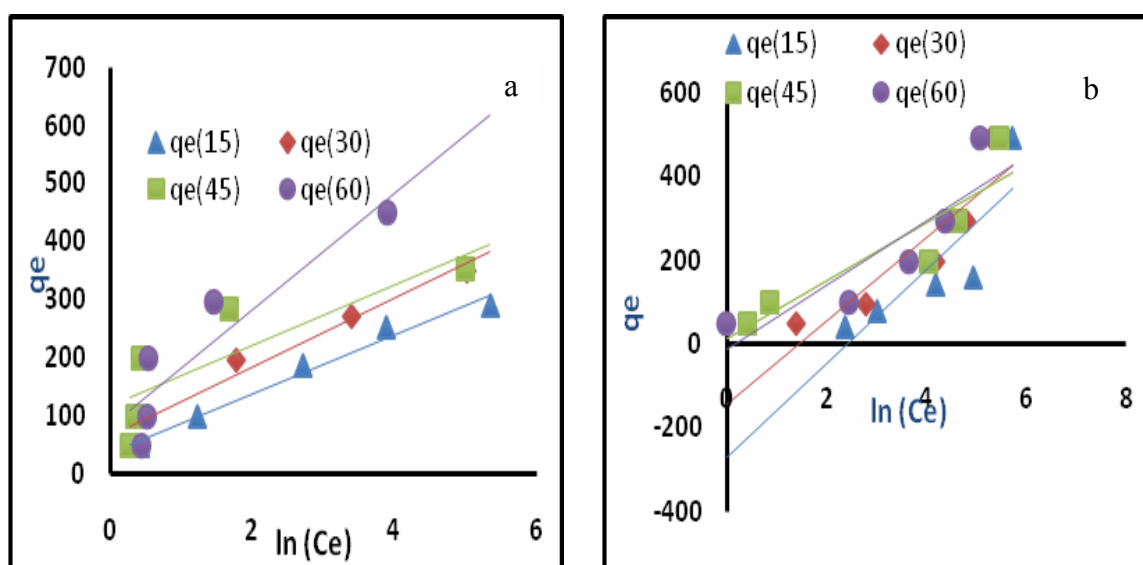


Fig. 18. Temkin isotherm model for Cr adsorption by (a) PANI and (b) CS-g-PANI.

Finally, **Table 6** represents comparison between different types of adsorbents used for the removal of Cr (VI) and our work. From the table we concluded that the maximum capacity of the

prepared adsorbents (polyaniline and chitosan-grafted polyaniline) represent the highest capacity of all the represented adsorbents.

**TABLE 5. Temkin adsorption isotherm parameters.**

resin	T°C	A	b (-)	Correlation Coefficient r <sup>2</sup>
PANI	15	2.0855	47.343	0.9801
	30	3.034	42.734	0.9668
	45	9.375	50.79	0.7015
	60	2.257	27.592	0.845
CS/PANI	15	11.167	21.36	0.7245
	30	4.187	25.223	0.8095
	45	1.1774	37.843	0.8205
	60	1.202	35.752	0.7595

**TABLE 6. Comparison between the maximum adsorption capacities of the prepared polymers with other adsorbents for Cr (VI).**

No.	Adsorbent	Q max(mg/g)	pH	Ref.
1	Glycine Modified	78		[41]
	Cross-linked			
	Chitosan			[42]
2	unmodified	90		
	groundnut hull			[42]
3	modified groundnut	131		
	hull			
4	rice husk carbon	47.61	2	[43]
5	treated waste	59.88	3	[44]
	newspaper			
6	peels of pea pod	4.33	2	[44]
7	Tea waste	7.29	2	[44]
8	Banana waste	10	2	[45]
9	Chitosan coated	33.27	5	[46]
	fly ash			
10	Guar gum-nano	55.56	7	[47]
	zinc oxide			
11	Wool	41.15	2	[48]
12	Olive cake	33.44	2	[48]
13	Saw dust	15.82	2	[48]
14	Almond	10.61	2	[48]
15	Mosamby peel	250	2	[49]
16	Mod.rice husk	278	2	[50]
17	Cs/CDTA/GO	166.98	3.5	[51]
18	PANI	526	2	This study
19	CS-g-PANI	370	2	This study

## Conclusion

Graft copolymerization was used for the preparation of chitosan-grafted-polyaniline) (CS-g-PANI). The conductive polymer, polyaniline (PAN) was also synthesized and used as a reference for the adsorption of chromium VI. The synthesized polymers were analyzed by means of FTIR, TGA, and TEM. The factor affected the adsorption processes were studied such as pH, time, temperature, and initial concentrations of chromium. Also, both kinetics and equilibrium isotherms were studied. The results indicated that the optimum conditions for the preparation of poly aniline are: APS to aniline ratio is 1.5, the HCL concentration is 2.5 M, the reaction time is 1.5h and the optimum ratio for the preparation of chitosan-grafted-poly aniline is CS/ANI is 1.2. It was also found that the prepared nanoparticles of PANI may reach a size of 23–32 nm and the CS-g-PANI is 26–37 nm. Equilibrium data of adsorption was in good agreement with Langmuire model with maximum adsorption capacity of 526 mg/g for PANI and 370 mg/g for CS-g-PANI at 60 °C. The adsorption mechanism was found to follow the second order model for the two resins.

## References

- Sud, D., Mahajan, G., Kaur, M.P., 2008. "Agricultural waste material as potential adsorbent for sequestering heavy metal ions from aqueous solutions - a review", *Bioresour. Technol.* 99, 6017–6027.
- Zare, E.N., Motahari, A., Sillanpaa M. Nanoadsorbents based on conducting polymer nanocomposites with main focus on polyaniline and its derivatives for removal of heavy metal ions/dyes: A review. *Environmental Research*, 162 (2018) 173–195.
- Demirbas, A., 2008. Heavy metal adsorption onto agro-based waste materials: a review. *J.Hazard. Mater.* 157, 220–229.
- Lakouraj, M.M., Hasanzadeh, F., Zare, E.N., 2014a. Nanogel and super-paramagnetic nanocomposite of thiacalix [4] arene functionalized chitosan: synthesis, characterization and heavy metal sorption. *Iran. Polym. J.* 23, 933–945.
- Lakouraj, M.M., Mojerlou, F., Zare, E.N., 2014b. "Nanogel and superparamagnetic nanocomposite based on sodium alginate for sorption of heavy metal ions", *Carbohydr. Polym.* 106, 34–41.
- Hua, M., Zhang, S., Pan, B., Zhang, W., Lv, L., *Egypt. J. Chem.* 63, No. 7 (2020)
- Zhang, Q., 2012. "Heavy metal removal from water/wastewater by nanosized metal oxides: a review". *J. Hazard. Mater.* 211–212, 317–331.
- Chang, M.Y.; Juang, R.S. "Adsorption of tannic acid, humic acid, and dyes from water using the composite of chitosan and activated clay", *J. Colloid Interface Sci.* 278 (2004) 18–25.
- El-Sayed, N.S.; Abd El-Aziz, M.E.; Kamel, S.; Turkey G. "Synthesis and characterization of polyaniline/tosylcellulose stearate composites as promising semiconducting materials" *Synthetic Metals*, 236 (2018), pp. 44–53
- Youssef, A.; Kamel, S.; El-Sakhawy, M.; and El Samahy, M. "Structural and electrical properties of paper–polyaniline composite", *Carbohydrate Polymers*, 90 (2012), pp. 1003–1007
- Darwish, A.; Ghoniem, A.; Hassaan, M.Y. "Synthesis and Characterization of Polyaniline/Mn<sub>3</sub>O<sub>4</sub>/Reduced Graphene Oxide Nanocomposite" *Egyptian Journal of Chemistry*, 2019
- Kumar, M.N.V.R., Muzzarelli, R.A.A., Muzzarelli, C., Sashiwa, H., and Domb, A.J., "Chitosan chemistry and pharmaceutical perspectives", *Chem. Rev.* 104 (2004) 6017–6084.
- Liu, K., Chen, L., Huang, L., and Lai, Y. "Evaluation of ethylenediamine-modified nanofibrillated cellulose/chitosan composites on adsorption of cationic and anionic dyes from aqueous solution", *Carbohydr. Polym.* 151 (2016) 1115–1119.
- Travlou, N.A., Kyzas, G.Z., Lazaridis, N.K., Deliyanni, E.A. "Functionalization of graphite oxide with magnetic chitosan for the preparation of ananocomposite dye adsorbent", *Langmuir* 29 (2013) 1657–1668.
- Prabhu, S.M., and Meenakshi, S. "Defluoridation of water using dicarboxylic acid mediated chitosan-polyaniline/zirconium biopolymeric complex", *Int. J. Biol. Macromol.* 85 (2016) 16–22.
- Ho, Y.S. and McKay, G. "Sorption of dye from aqueous solution by peat", *Chem. Eng. J.*, 70(1998) 115–124.
- Ho, Y.S. and McKay, G. "A kinetic study of dye sorption by biosorbent waste product pith", *Resour. Conserv. Recycling*, 25(1999) 171–193.
- Allen, S.J. Gan, Q. Matthews R., Johnson P.A. "Comparison of optimised isotherm models for basic dye adsorption by kudzu", *Bioresour Technol* 88(2003) 143–152.

18. Foo, K.Y. Hameed, B.H. "Insights into the modeling of adsorption isotherm systems", *Chem. Eng. J.* 156 (2010) 2–10.
19. Irving Langmuir, "The constitution and fundamental properties of solids and liquids", Part I. Solids, *J. Am. Chem. Soc.* 38 (11) (1916) 2221–2295.
20. Singh, S. Barick, K.C., Bahadur D. "Surface engineered magnetic nanoparticles for removal of toxic metal ions and bacterial pathogens", *J. Hazard. Mater.* 192(2011) 1539–1547.
21. Temkin, M.J., Pyzhev, V. "Recent modifications to Langmuir isotherms", *Acta Physiochim. USSR* 12 (1940) 217-222.
22. Bhadra, S., Singha, N. K., Chattopadhyay, S., Khastgir, D. "Effect of different reaction parameters on the conductivity and dielectric properties of polyaniline synthesized electrochemically and modeling of conductivity against reaction parameters through regression analysis. *Journal of Polymer Science Part B: Polymer Physics*, 45(15) (2007b), 2046-2059.
23. Han, M. G., Cho, S. K., Oh, S. G., Im, S. S. "Preparation and characterization of polyaniline nanoparticles synthesized from DBSA micellar solution", *Synth. Met.* (2002), 126, 53.
24. Minisy, I. M., Salahuddin, N. A., Ayad, M. M. "Chitosan/polyaniline hybrid for the removal of cationic and anionic dyes from aqueous solutions", *J. APPL. POLYM. SCI.* (2019) DOI: 10.1002/APP.47056
25. Ismail, Y. A., Shin, S. R., Shin, K. M.; Yoon, S. G., Shon, K., Kim, S. I. Sens. "Electrochemical actuation in chitosan/polyaniline microfibers for artificial muscles fabricated using an in situ polymerization", *Actuators B.* 129 (2008) 834.
26. Govindan, S., Nivethaa, E. A. K.; Saravanan, R., Narayanan, Stephen, V. "Synthesis and characterization of chitosan–silver nanocomposite", *A. Appl. Nanosci.*, 2 (2012) 299.
27. Khan, R., Dhayal, M. Biosens. »Chitosan/polyaniline hybrid conducting biopolymer base impedimetric immunosensor to detect Ochratoxin-A", *Bioelectron* 24 (2009) 1700.
28. Hosseini, S. H., Simiari, J., Farhadpour, B. "Chemical and electrochemical grafting of polyaniline onto chitosan", *Iranian Polymer Journal*, 18(2009)3-13.
29. Shi, L., Wang, X., Lu, L., Yang, X., Wu, X. "Preparation of TiO<sub>2</sub>/polyaniline nanocomposite from a lyotropic liquid crystalline solution", *Synthetic Metals*, 159 (2009), 2525-2529.
30. Yu, L., He, Y., Bin, L., Yue's, F." Study of Radiation-Induced Graft Copolymerization of Butyl Acrylate onto Chitosan in Acetic Acid Aqueous Solution *Journal of Applied Polymer Science*, 90 (2003), 2855.
31. Tiwari, A., Singh, V. "Synthesis and characterization of electrical conducting chitosan-graft-polyaniline", *EXPRESS Polym. Lett.*, 1 (2007) 308–317.
32. Kang, H.M., Cai, Y.L., Liu, P.S. "Synthesis, characterization and thermal sensitivity of chitosan-based graft copolymers", *Carbohydrate Research* 341(2006) 2851.
33. Kumara, P.A., Rayb, M., Chakraborty, S. "Hexavalent chromium removal from wastewater using aniline formaldehyde condensate coated silica gel", *Journal of Hazardous Materials* 143 (2007) 24–32.
34. Karthik, R., "Facile synthesis of cross linked-chitosan-grafted-polyaniline composite and its Cr(VI) uptake studies", *International Journal of Biological Macromolecules* 67(2014)210-219.
35. Chagas, P. M. B., Carvalho, L. B., Francisco, A. A. C., Nogueira, G. E., Guimarães, A. D. C. R. "Nanostructured oxide stabilized by chitosan: Hybrid composite as an adsorbent for the removal of chromium (VI)", *Journal of Environmental Chemical Engineering* 6 (2018) 1008–101.
36. Ozdemir, E., Duranoğlu, D., Beker, U., Avcı, A. "Process optimization for Cr (VI) adsorption onto activated carbons by experimental design" *Chemical Engineering Journal* 172 (2011) 207 – 218,
37. Oyedoh, E. A., Ekwonu, M., "Experimental investigation on chromium(VI) removal from aqueous solution using activated carbon resorcinol formaldehyde xerogels" *Acta Polytechnica.* 56(2016) 373-378.
38. Kamari, A., Ngah, W.S.W., Liew, L.K., "Chitosan and chemically modified chitosan beads for acid dyes sorption", *J. Environ. Sci.* 21 (2009) 296–302.
39. Atun, G., Hisarlı, G. "Adsorption of carminic acid, a dye on glass powder", *Chem. Eng. J.* 95 (2003) 241–249.
40. Kannan, D., Khodaverdi, R., Olfat, L., Jafarian, *Egypt. J. Chem.* 63, No. 7 (2020)

- A. and Diabat, A., "Integrated fuzzy multi criteria decision making method and multi-objective programming approach for supplier selection and order allocation in a green supply chain", *Journal of Cleaner Production*, 47(2013), 355-367.
41. Hamouda, A. S., Ahmed, S. A., Mohamed, N.M., Khalil, M.M.H. "Adsorption of Chromium(VI) from Aqueous Solution by Glycine Modified Cross-linked Chitosan Resin", *Egypt. J. Chem.* 61 (5) (2018) 799 - 812.
42. Owalude, S. O., Tella, A. C. "Removal of hexavalent chromium from aqueous solutions by adsorption on modified groundnut hull", *Benisuef university journal of basic and applied sciences*, 5 (2016) 377-388
43. Khan, T., Isa M. H., Mustafa M. R.U., Yeek, H., Baloo L., Abd Manana T.S.B., et al. "Cr(VI) adsorption from aqueous solution by an agricultural waste based carbon", *RSC Adv*, 6 (2016) 56365-56374
44. Dehghani, M.H., Sanaei, D., Ali I., Bhatnagar A. "Removal of chromium(VI) from aqueous solution using treated waste newspaper as a low-cost adsorbent: kinetic modeling and isotherm studies", *J Mol Liquids* 215 (2016) 671-679.
45. Sharma, P.K., Ayub, S., Tripathi, CN. "Isotherms describing physical adsorption of Cr(VI) from aqueous solution using various agricultural wastes as adsorbents", *Cogent Eng.* 3 (2016) 1-20.
46. Wen, Y., Tang, Z., Chen, Y., Gu, Y. "Adsorption of Cr(VI) from aqueous solutions using chitosan-coated fly ash composite as biosorbent" *Chem Eng J* 175 (2011) 110-16.
47. Khan, T.A., Nazir, M., Ali, I., Kumar, A. "Removal of chromium(VI) from aqueous solution using guar gum-nano zinc oxide biocomposite adsorbent", *Arabian J Chem* (2013).
48. Dakiky, M., Khamis, M., Manassra, A., Mer'eb, M. "Selective adsorption of chromium(VI) in industrial wastewater using low-cost abundantly available adsorbents" *Adv Environ Res.* 6 (2002) 533-40.
49. Saha, R., Mukherjee, K., Saha, I., Ghosh, A., Ghosh, S.K., Saha, B. "Removal of hexavalent chromium from water by adsorption on mosambi (*Citrus limetta*) peel", *Res. Chem. Intermed.* 39 (2013) 2245-57.
50. El-Shafey, E.I. "Behaviour of reduction-sorption of chromium(VI) from an aqueous solution on a modified sorbent from rice husk", *Water Air Soil Pollut* 163 (2005) 81-102.
51. Mohamed, E.A., Ali, "Synthesis and adsorption properties of chitosan-CDTA-GO nanocomposite for removal of hexavalent chromium from aqueous solutions", *Arabian Journal of Chemistry* 11 (7) (2018), 1107-1116